Int. J. Heat Mass Transfer. Vol. 22, pp. 721–729

0017–9310/79/0501-0721 $02.00/0

INFLUENCE OF SLIP VELOCITY AT A MEMBRANE SURFACE ON ULTRAFILTRATION PERFORMANCE—I. CHANNEL FLOW SYSTEM

RAJINDAR SINGH and ROBERT L. LAURENCE
Department of Chemical Engineering, University of Massachusetts, Amherst, MA 01003, U.S.A.

(*Received* 1 *August* 1977 *and in revised form* 24 *August* 1978)

Abstract—The influence of slip-velocity at a porous surface is studied in detail for a parallel flat membrane system assuming fully-developed flow. The effect of slip coefficient on velocity profiles, pressure gradient and concentration polarization in ultrafiltration is examined. The equations of motion are solved by the regular perturbation method. The coupled diffusion equation in the boundary layer is solved using a finite difference scheme.

NOMENCLATURE

A_j, B_j, E_j, F_j, coefficients in the matrix equations;
c, solute concentration;
c_0, inlet solute concentration;
c_w, solute concentration at membrane surface;
$\bar{c} = c_0/(1-\xi)$, mixing-cup average solute concentration;
C, c/c_0;
C_p, $c_w/\bar{c} - 1$, concentration polarization;
$(C_p)_\phi/(C_p)_{\phi=0}$, normalized concentration polarization;
D, solute diffusivity;
h, half-width of channel;
k, membrane permeability;
K, an integration constant;
p_x, pressure in the channel at a given value of x;
p_0, inlet pressure in channel;
P, $(p_0 - p_x)/(\rho \bar{u}_0^2/2)$;
Pe, $v_w h/D$, Peclet number;
Re, $4\bar{u}_0/\nu$, Reynolds number for flow entering the channel;
Re_w, $v_w h/\nu$, wall Reynolds number;
u, velocity component in x-direction;
$\bar{u}_0$, average velocity over the channel at channel inlet;
$\bar{u}$, average velocity over the channel at a given value of x;
U, $u/\bar{u}_0$;
u_s^0, $(u/\bar{u}_0)_{y=h}$, normalized slip velocity;
u_s, $(u/\bar{u})_{y=h}$, normalized slip velocity;
v, velocity component in y-direction;
v_w, velocity of fluid through membrane;
V, v/v_w;
x, axial distance from channel entrance;
y, distance normal to phase boundary.

Greek symbols

α_0, $1/Pe$, normalized diffusion coefficient;
α, surface characteristic of membrane;
β_j, γ_j, parameters used in numerical calculations;
ε, $V_w/\bar{u}_0$;
λ, y/h;
μ, viscosity;
ν, kinematic viscosity;
ξ, $v_w x/\bar{u}_0 h = 4Re_w x/Reh$, fraction of water removed at a given value of x;
ρ, solution density;
ϕ, $k^{1/2}/\alpha h$, slip coefficient;
ψ, stream function.

Superscripts

$'$, $''$, $'''$, 1st, 2nd and 3rd-order derivatives.

1. INTRODUCTION

THE HIGH flux nature of the skin type, anisotropic ultrafiltration membranes results in the rapid build-up of solutes at the membrane surface leading to the formation of a polarized gel-layer. This phenomena, often referred to as concentration polarization, is highly flux-limiting and, consequently, has been studied extensively [4, 7].

Brian [5] solved the problem of concentration polarization for low molecular weight solutes (reverse osmosis) assuming laminar flow in a channel with parallel flat membranes. Infinite-series and finite difference solutions of the diffusion equation in the boundary layer were obtained. The results of the two solutions were in excellent agreement. In order to solve the diffusion equation, the velocity field must first be specified. Brian used the solution of Berman [3], modified to exclude the terms containing the wall Reynolds number which is negligibly small for

reverse osmosis. In ultrafiltration, where the flux rates are considerably higher, wall Reynolds number is not negligible and, hence, cannot be ignored.

Berman obtained a first-order perturbation solution for the velocity field in the case of a homogeneous fluid flowing between parallel porous walls with a uniform withdrawal flux through the wall. In his analysis he tacitly assumed the zero-slip boundary condition which characterizes flows with solid bounding walls. Beavers and Joseph [1], however, showed the existence of a slip velocity at a porous surface on the basis of theoretical arguments and experimental verification. In later studies, Beavers *et al.* [2] and Kohler [6] showed that their experimental results agreed remarkably well with analytical predictions, thus lending further support to the slip flow model.

The present work is an attempt to study the effect of non-zero tangential velocity (the so-called slip velocity) on velocity field, pressure gradient and concentration polarization in ultrafiltration processing. The ramifications of slip velocity in predicting flux rates in ultrafiltration are examined.

The equations of motion in two-dimensions are solved by a first-order perturbation method assuming slip velocity at the membrane surface. The diffusion equation is solved by a finite difference technique. The results of the solutions are discussed in Section 4 and the conclusions are presented in Section 5. Analysis of the tubular flow system is given in a subsequent paper [11].

2. MATHEMATICAL FORMULATION

2.1. *The equations of motion*

Consider a case in which fluid containing macromolecular solutes flows within the channel between two parallel, flat ultrafiltration membranes, as shown in Fig. 1. The width of the membranes is assumed to be very large relative to the membrane spacing, and product water is assumed to be permeating both the upper and the lower membranes; thus the flow will be assumed to be two-dimensional and symmetrical about the midplane of the channel of half-thickness h. This implies that the flow is assumed to be laminar, and natural convection effects are assumed to be negligible. It is also assumed that fluid is incompressible and operation is steady-state.

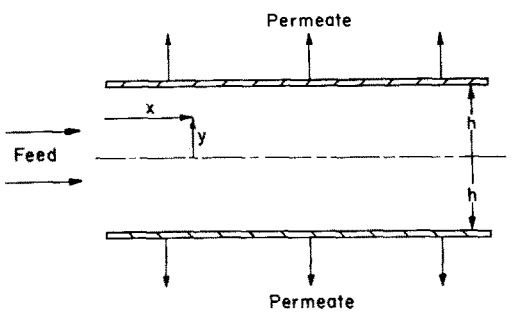

FIG. 1. Parallel flat membranes.

Under the assumed conditions, the pertinent equations of linear momentum and continuity with the requisite boundary conditions are:

$$u\frac{\partial u}{\partial x}+\frac{v}{h}\frac{\partial u}{\partial \lambda}=-\frac{1}{\rho}\frac{\partial p}{\partial x}+\nu\left(\frac{\partial^2 u}{\partial x^2}+\frac{1}{h^2}\frac{\partial^2 u}{\partial \lambda^2}\right), \quad (1)$$

$$u\frac{\partial v}{\partial x}+\frac{v}{h}\frac{\partial v}{\partial \lambda}=-\frac{1}{\rho h}\frac{\partial p}{\partial \lambda}+\nu\left(\frac{\partial^2 v}{\partial x^2}+\frac{1}{h^2}\frac{\partial^2 v}{\partial \lambda^2}\right), \quad (2)$$

$$\frac{\partial u}{\partial x}+\frac{1}{h}\frac{\partial v}{\partial \lambda}=0, \quad (3)$$

$$u(x,\pm 1)=-\frac{k^{1/2}}{\alpha h}\left(\frac{\partial u}{\partial \lambda}\right), \quad (4)$$

$$\left(\frac{\partial u}{\partial \lambda}\right)_{\lambda=0}=0, \quad (5)$$

$$v(x,0)=0, \quad (6)$$

$$v(x,\pm 1)=v_w, \quad (7)$$

where

$$\lambda=\frac{y}{h}.$$

Equation (4) is the slip-flow boundary condition of Beavers and Joseph [1]. The slip velocity at the membrane surface is proportional to the shear rate at the permeable boundary. This slip velocity is connected with the presence of a thin layer of streamwise moving fluid in the boundary region just below the permeable surface. The fluid in this layer is considered to be pulled along by the flow above the porous surface. $\phi(=k^{1/2}/\alpha h)$ is the slip coefficient where k is the permeability of the membrane matrix, and α is a dimensionless constant dependent on the surface characteristics of the membrane. When $k=0$, equation (4) reduces to the no-slip condition appropriate to a solid wall.

Equation (7) is the condition for constant permeation flux. It is assumed that this is valid. No solutions have been obtained and/or reported for variable permeation flux along the longitudinal position for high wall Reynolds numbers.

For a two-dimensional incompressible flow, a stream function $\psi(x,\lambda)$ exists such that,

$$u(x,\lambda)=\frac{1}{h}\frac{\partial \psi}{\partial \lambda}, \quad (8)$$

$$v(x,\lambda)=-\frac{\partial \psi}{\partial x}, \quad (9)$$

and the continuity equation (3) is satisfied.

A suitable choice of stream function is,

$$\psi(x,\lambda)=[h\bar{u}_0-v_w x]f(\lambda), \quad (10)$$

giving for the velocity components by equations (8) and (9),

$$u(x,\lambda)=\left[\bar{u}_0-\frac{v_w x}{h}\right]f'(\lambda), \quad (11)$$

$$v(\lambda)=v_w f(\lambda). \quad (12)$$

In these equations $f(\lambda)$ is some function yet to be determined. Under the assumption of constant permeation flux v_w, the y component of velocity, v, becomes a function of λ only. Using the standard analysis, equations (1) and (2) can be rephrased:

$$\frac{d}{d\lambda}\left[\frac{v_w}{h}\left(f'^2 - ff'' + \frac{1}{Re_w}f'''\right)\right] = 0, \quad (13)$$

where

$$Re_w = \frac{v_w h}{\nu}.$$

This equation can be integrated to

$$Re_w(f'^2 - ff'') + f''' = K, \quad (14)$$

where K is the constant of integration.

The new set of boundary conditions is similarly obtained by substituting equations (11) and (12) in equations (4)–(7). Thus

$$f'(1) = -\phi f''(1), \quad (15)$$

$$f''(0) = 0, \quad (16)$$

$$f(0) = 0, \quad (17)$$

$$f(1) = 1. \quad (18)$$

Equation (14) is the so-called Falkner–Skan equation. The solution using these boundary conditions is described in Section 3.1.

2.2. *The diffusion equation*

It is assumed that the solute concentration is uniform over the channel cross-section at the channel inlet. As the solution flows down the channel and permeate is removed through the membranes, a solute-concentration profile develops and the solute concentration at the membrane surface increases along the length of the channel. Assuming steady-state operation and both diffusion and convection of solute in the transverse and longitudinal directions, a solute material balance on a differential volume element yields the following partial differential equation (in dimensionless form)

$$U\frac{\partial C}{\partial \xi} + V\frac{\partial C}{\partial \lambda} = \frac{1}{Pe}\left(\frac{\partial^2 C}{\partial \lambda^2} + \varepsilon^2\frac{\partial^2 C}{\partial \xi^2}\right), \quad (19)$$

where

$$U = \frac{u}{\bar{u}_0}, \quad V = \frac{v}{v_w}, \quad C = \frac{c}{c_0}, \quad \lambda = \frac{y}{h},$$

$$\xi = \frac{v_w}{\bar{u}_0}\cdot\frac{x}{h} = \frac{4Re_w}{Re}\cdot\frac{x}{h}, \quad Pe = \frac{v_w h}{D},$$

$$\varepsilon = \frac{v_w}{\bar{u}_0}, \quad Re = \frac{4\bar{u}_0 h}{\nu}.$$

For $v_w \ll \bar{u}_0$, ε^2 is very small and hence the second term on the right-hand side of equation (19) is negligible. This shows that diffusion in the longitudinal direction is negligibly small. Equation (19) can then be rewritten as:

$$U\frac{\partial C}{\partial \xi} + V\frac{\partial C}{\partial \lambda} = \alpha_0\frac{\partial^2 C}{\partial \lambda^2}, \quad (20)$$

where

$$\alpha_0 = \frac{1}{Pe}.$$

The boundary conditions are:

$$C(0, \lambda) = 1, \quad (21)$$

$$\left(\frac{\partial C}{\partial \lambda}\right)_{\lambda=0} = 0, \quad (22)$$

$$C(\xi, 1) = \alpha_0\left(\frac{\partial C}{\partial \lambda}\right)_{\lambda=1}. \quad (23)$$

Equation (23) is the so-called gel polarization model. It assumes that the membrane is completely retentive to solute and that the convective flow of solute to the membrane surface is equal to the diffusive back-transport of solute from the concentrated polarized layer to the bulk-solution. This steady state is reached in less than a minute [4].

The solution of equation (20) with the appropriate boundary conditions is reported in the Appendix incorporating the results of velocity profiles U and V, obtained from Section 3.1.

3. METHODS OF SOLUTION

3.1. *The perturbation solution*

The third-order, nonlinear, ordinary differential equation (14), suggests a perturbation solution if the perturbation parameter Re_w, is small. Equations exhibiting certain essential features like nonlinearities often preclude exact analytical solutions. Even if the exact solution of a problem can be found explicitly, it may be useless for mathematical and physical interpretation or numerical evaluation. Thus, in order to obtain information about solutions of equations, we are forced to resort to approximations, numerical solutions or combinations of both. Foremost among the approximation methods are regular perturbation methods (see, e.g. Nayfeh [8]). According to these techniques, the solution is represented by the first few terms of a perturbation expansion, usually not more than two terms. The expansions may be carried out in terms of a parameter which appears naturally in the equations—e.g. the wall Reynolds number, Re_w, in this case—or which can be artificially introduced for convenience.

The solution of equation (14) for small Re_w may be expressed in a power series as

$$f(\lambda) = f_0(\lambda) + f_1(\lambda)Re_w + f_2(\lambda)Re_w^2 + f_3(Re_w^3) + \ldots \quad (24)$$

and

$$K = K_0 + K_1 Re_w + K_2 Re_w^2 + K_3 Re_w^3 + \ldots \quad (25)$$

Here the f_n's and K_n's are taken to be independent of Re_w. Substituting equations (24) and (25) in equation (14) and collecting terms of like powers of Re_w leads to the following set of equations:

zero order:

$$f_0''' = K_0, \quad (26)$$

first order:

$$f_1''' = K_1 - f_0'^2 + f_0 f_0'', \tag{27}$$

second order:

$$f_2''' = K_2 + f_0 f_1'' + f_1 f_0'' - 2f_0' f_1'. \tag{28}$$

The boundary conditions to be satisfied by the f_n's are from equations (15)–(18):

$$f_n'(1) + \phi f_n''(1) = 0, \tag{29}$$

$$f_n(0) = f_n''(0) = 0, \tag{30}$$

$$\begin{aligned} f_0(1) &= 1, \\ f_n(1) &= 0, \end{aligned} \quad \text{for } n \geqslant 1. \tag{31}$$

Equations (26)–(28) are ordinary, linear, third-order equations which are readily solved to give successive approximations to $f(\lambda)$.

The first-order perturbation solution gives for $f(\lambda)$ and K:

$$f(\lambda) = (b_1\lambda^3 + b_2\lambda) - \frac{Re_w}{280}(c_1\lambda^7 + c_2\lambda^3 + c_3\lambda) \tag{32}$$

and

$$K = -3c_1^{1/2} + \frac{9Re_w c_4}{35}, \tag{33}$$

where b_1, b_2, c_1, c_2, c_3 and c_4 are functions of ϕ and are defined in the Appendix.

For the no-slip velocity case, that is, when $\phi = 0$, equations (32) and (33) reduce to the solution of Berman [3]. Berman, using a second-order perturbation calculation, found the coefficient of Re_w^2 in K to be 0.02. Thus, a first-order solution is acceptable.

The velocity profiles are obtained by substituting equation (32) in equations (11) and (12). Hence

$$U = \left(1 - \frac{4Re_w}{Re}\cdot\frac{x}{h}\right)\left[(3b_1\lambda^2 + b_2) - \frac{Re_w}{280}(7c_1\lambda^6 + 3c_2\lambda^2 + c_3)\right], \tag{34}$$

$$V = (b_1\lambda^3 + b_2\lambda) - \frac{Re_w}{280}(c_1\lambda^7 + c_2\lambda^3 + c_3\lambda). \tag{35}$$

Normalized axial component of velocity can be readily attained from equation (34) to give

$$\frac{u}{\bar{u}} = (3b_1\lambda^2 + b_2) - \frac{Re_w}{280}(7c_1\lambda^6 + 3c_2\lambda^2 + c_3), \tag{36}$$

where

$$\bar{u} = \frac{1}{2}\int_{\lambda=-1}^{\lambda=1} u(\lambda)\,d\lambda = 1 - \frac{4Re_w}{Re}\cdot\frac{x}{h} = 1 - \xi. \tag{37}$$

Normalized pressure gradient P, is obtained from equations (1) and (2) and (14) as

$$P = \frac{p_0 - p_x}{\frac{1}{2}\rho\bar{u}_0^2} = -\frac{2K}{Re}\left[\frac{x}{h} - \frac{2Re_w}{Re}\left(\frac{x}{h}\right)^2\right]. \tag{38}$$

3.2. *The finite difference solution*

The diffusion equation in the concentration boundary layer (20), with the velocity field obtained from equations (34) and (35), is solved by a finite difference scheme implicit in λ. The solution procedure is outlined in the Appendix.

4. RESULTS AND DISCUSSION

4.1. *Velocity profiles*

Figure 2 is a plot of $u/\bar{u}_0$ vs λ for an entrance Reynolds number of 1000 and a longitudinal position x/h, equal to 500. The curves are plotted for slip coefficient, ϕ equal to 0, 0.1 and 0.5, and a wall Reynolds number, Re_w of 0.1. According to Kohler [6], values of ϕ up to 0.5 are reasonable. As expected, the velocity at the membrane surface ($\lambda = 1$) is 0 when ϕ is 0. As the slip velocity increases with increasing ϕ, the wall shear decreases and the profiles become flatter, approaching those for plug flow.

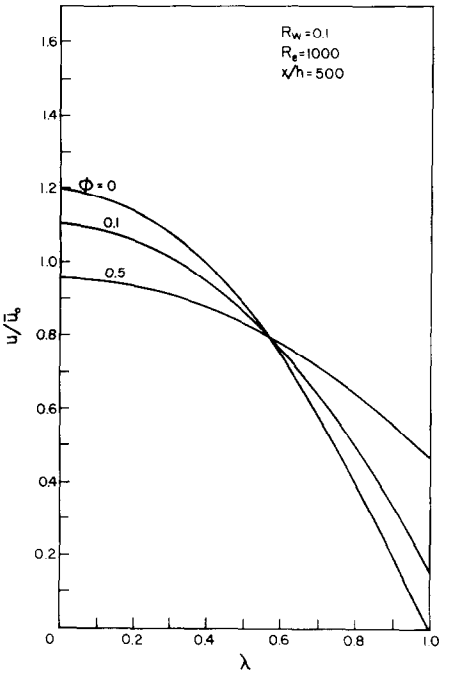

FIG. 2. Velocity profiles for $Re_w = 0.1$ based on entrance Reynolds number for channel flow.

Evidence of the effect of ϕ on normalized slip velocity u_s^0 is shown in Fig. 3. u_s^0 increases with ϕ and appears to approach an asymptotic value. u_s^0 decreases as x/h increases indicating that at a point further downstream, the slip velocity is decreased. A similar plot at a wall Reynolds number of 0.2 is also shown. It is easily seen that u_s^0 is considerably reduced when Re_w increases from 0.1–0.2.

Velocity profiles in the form $u/\bar{u}$ vs λ are plotted in Fig. 4. This is similar to that for $u/\bar{u}_0$ vs λ except that it is independent of entrance Reynolds number and longitudinal position. This is evident from equation (36). The velocity profiles are essentially independent of wall Reynolds number except when $Re_w = 5$. It is clear from Fig. 5 that u_s increases with Re_w and ϕ.

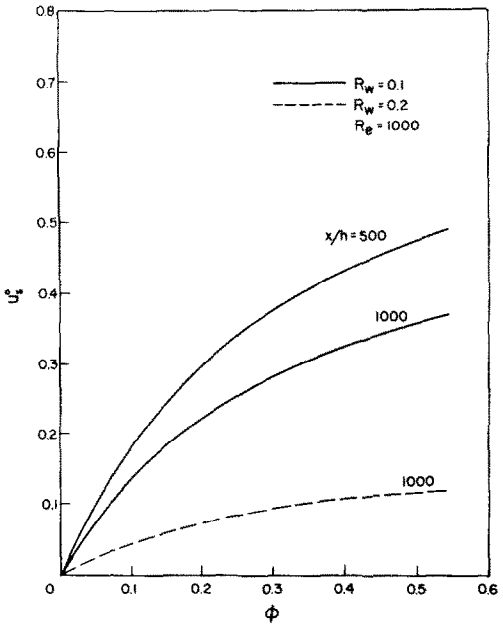

FIG. 3. Effect of slip coefficient on normalized slip velocity for $Re_w = 0.1$ and 0.2 based on entrance Reynolds number for channel flow.

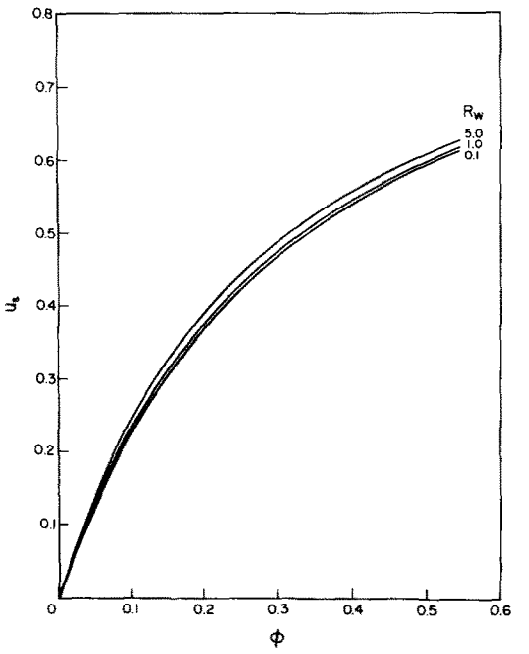

FIG. 5. Effect of slip coefficient on normalized slip velocity for $Re_w = 0.1$, 1.0 and 5.0.

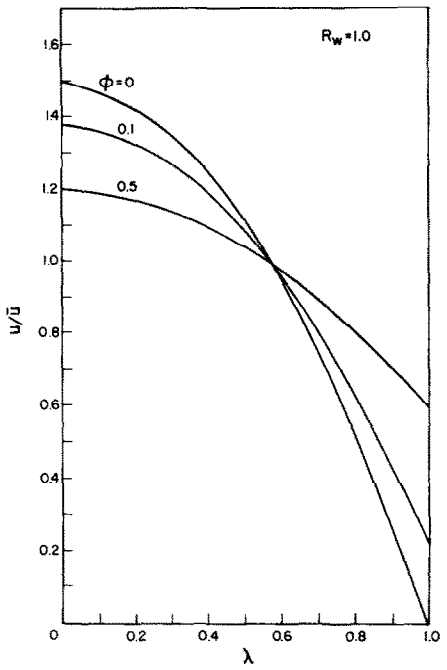

FIG. 4. Velocity profiles for $Re_w = 1.0$ for channel flow.

The increase in u_s for an increase in Re_w from 0.1–1 is negligibly small. However, there is a significant shift at an $Re_w = 5$. u_s approaches an asymptotic value as ϕ increases indicating an upper bound on ϕ.

4.2. *Pressure gradient*

Inspection of Fig. 6 reveals that the magnitude of pressure gradient P, increases with x/h for an entrance Reynolds number equal to 1000. The effect of slip coefficient ϕ, at the porous (membrane) surface is to decrease P, and the larger the value of ϕ, the greater the reduction in the value of P. This behavior is connected with the diminution in the shear stress at the membrane surface which, in turn, is a consequence of the fact that the velocity no longer need be zero at that surface. As was observed in the case of velocity profiles, an increase in Re_w would result in a decrease in shear stress so that P would also decrease.

4.3. *Concentration polarization*

Figure 7 presents the results of the finite difference solution, plotted in a manner suggested by Brian [5] for $\phi = 0$ and $Re_w = 0.2$ with $\alpha_0 = 0.1$, 0.2, 0.5, 1.0 and 2.0. The plot agrees very well with that of Brian except when $\alpha_0 = 0.1$, which indicates a higher value of concentration polarization C_p. This is because the effect of wall Reynolds number has not been ignored. When Re_w is not negligibly small, that is, for ultrafiltration membranes which have high flux rates, there is rapid convection of solutes to the membrane surface resulting in an increase in C_p. This difference is insignificant for $\alpha_0 = 0.2$ and disappears completely for higher values of α_0.

For any value of α_0, C_p is seen to increase with the fraction of water removed (or longitudinal position) ξ, and then to level out at an asymptotic value of C_p. The asymptote corresponds to the far-downstream solution for the polarization, and it is approached at relatively low values of ξ when α_0 is large. In contrast, at low values of α_0, the asymptotic polarization is approached only as ξ nears unity. When the value of C_p is substantially below the asymptotic value, the solution corresponds to the entrance region solution. Similar plots for $\phi = 0.1$

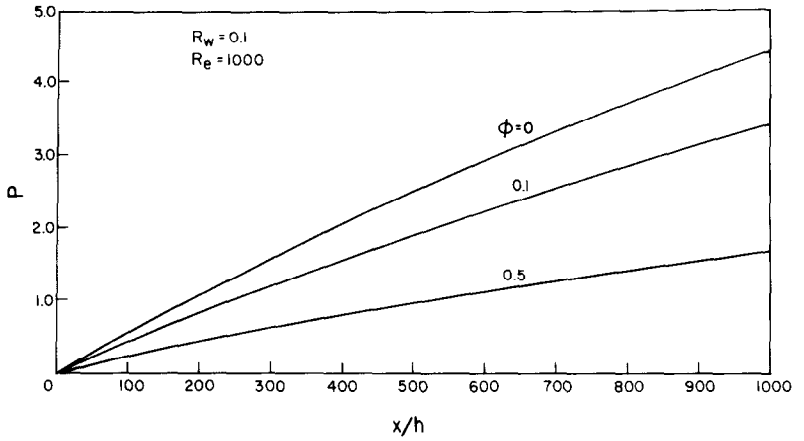

FIG. 6. Effect of slip coefficient on axial pressure gradient for $Re_w = 0.1$.

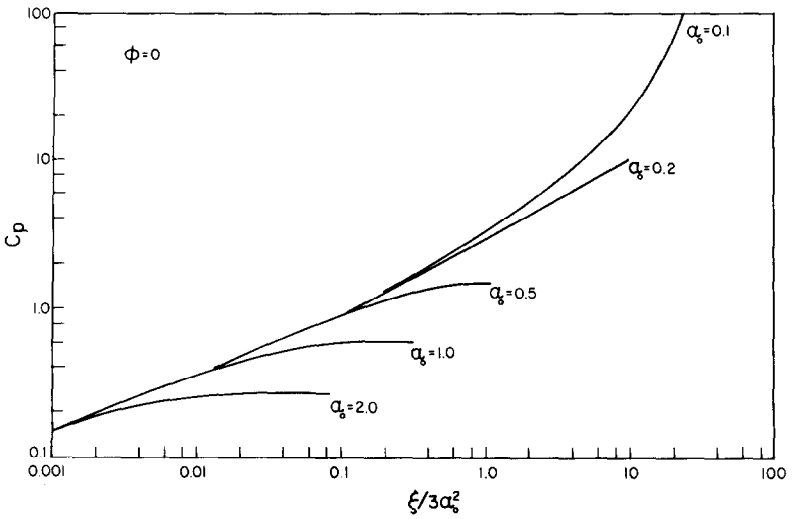

FIG. 7. Concentration polarization as a function of fraction of water removed (or longitudinal position) ξ, for $\phi = 0$.

and 0.5 are shown in Figs. 8 and 9, respectively. The effect of ϕ is to decrease the value of C_p, this decrease being more significant when α_0 is small. Thus, the value of C_p when $\phi = 0.5$ is lower as compared to when $\phi = 0$ for a particular value of α_0. The pronounced effect of ϕ when α_0 is small is due to the fact that changes in both parameters result in similar responses. This is discussed in detail below.

The effect of ϕ can be further observed from Fig. 10 which is a plot of $(C_p)\phi/(C_p)_{\phi=0}$ vs ϕ for $\alpha_0 = 0.1$, 0.2, 0.5, 1.0 and 2.0 when $\xi = 0.10$ and 0.60. For any value of α_0, the normalized polarization seen to decrease with increase in ϕ, and the decrease is significant when α_0 is small. Thus, the reduction in $(C_p)\phi/(C_p)_{\phi=0}$ is nearly five-fold when $\alpha_0 = 0.1$ as compared to a slightly more than one-fold reduction when $\alpha_0 = 2.0$ at $\phi = 0.5$ and $\xi = 0.60$. It is to be noted that the effect of ϕ on polarization is similar to that of α_0 suggesting a possible reason for the effect of ϕ on reduction of polarization. An increase in the value α_0 indicates an increase in the value of the diffusion coefficient D, that is, an increase in back-diffusion of solute from the membrane surface for the same values of v_w and h. It follows from this that slip velocity at the membrane surface promotes back-diffusion resulting in a lower value of C_p and, consequently, a higher value of flux rate.

Possible explanations for slip-velocity-induced back diffusion are:

(1) that the velocity profiles are flatter due to a decrease in the velocity gradient at the membrane surface; and

(2) that the fluid in the boundary region just below the permeable surface is pulled along by flow above the porous surface, thus, enhancing diffusion of solutes.

The effect of ξ on normalized polarization is also shown in Fig. 10. Thus, when 10% of the water is removed ($\xi = 0.10$), the normalized polarization has a lower value as compared to when $\xi = 0.60$. When $\alpha_0 = 0.1$, however, the trend is reversed. This is due to the fact that polarization for $\phi = 0$ is very large

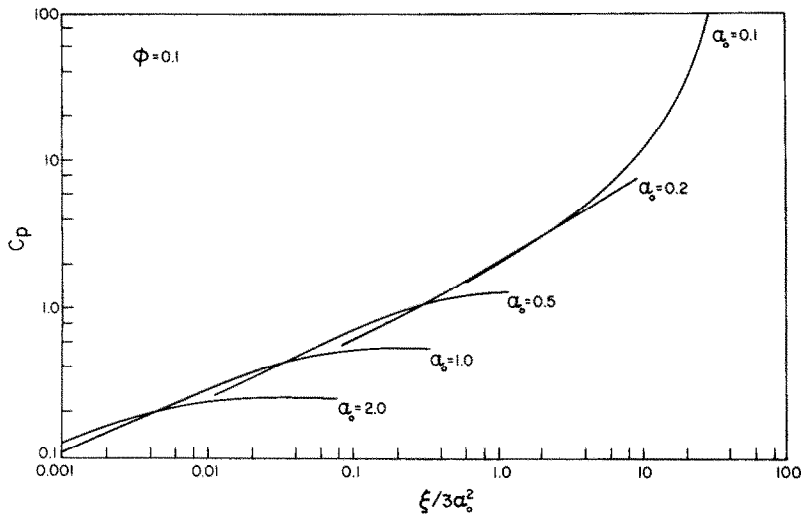

FIG. 8. Concentration polarization as a function of fraction of water removed (or longitudinal position) ξ, for $\phi = 0.1$.

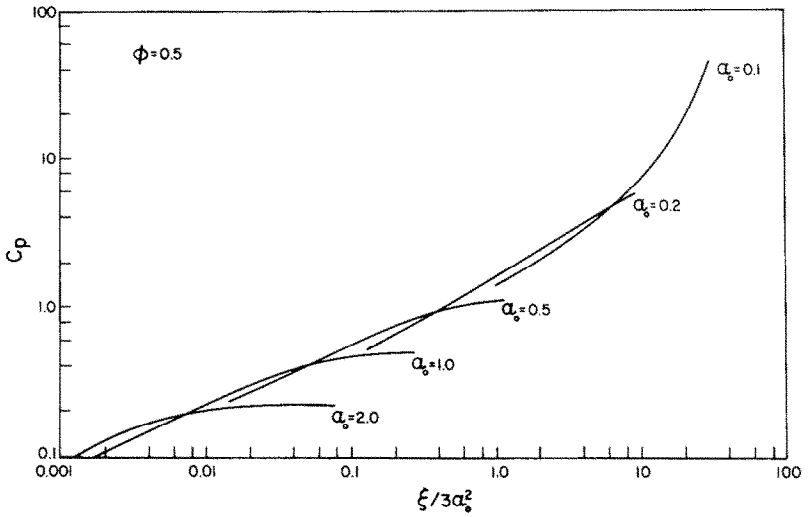

FIG. 9. Concentration polarization as a function of fraction of water removed (or longitudinal position) ξ, for $\phi = 0.5$.

when $\xi = 0.60$ as compared to when $\xi = 0.10$, and α_0 due to its low value has very little effect on reducing polarization.

5. CONCLUSIONS

The present study provides fundamental information for the analysis of ultrafiltration systems. The velocity profiles flatten and approach plug flow as the slip coefficient increases due to a decrease in the wall shear rate. Slip velocity increases with slip coefficient and approaches an asymptotic value. Concentration polarization at the membrane surface is reduced as slip coefficient increases and the effect is more significant for low values of the normalized diffusion coefficient. It is observed that the effect of slip coefficient on polarization is to promote diffusive transport of solute molecules from the membrane surface to the bulk solution. The net effect of this is to reduce polarization and increase flux rates through the membrane. Typical values indicating one to three fold decrease in polarization with slip coefficient are shown in Table 1.

Table 1. Effect of slip coefficient on concentration polarization

ξ	ϕ	α_0	$\bar{C}_p$	C_p^*
0.25	0	0.1	17.0	46.0
		1.0	0.59	0.6
	0.1	0.1	10.0	25.0
		1.0	0.52	0.55
	0.5	0.1	6.5	13.5
		1.0	0.44	0.49

*C_p is the average concentration polarization over the length of the membrane channel and it corresponds to when 50% of the water has been removed, that is, when the average value of ξ is equal to 0.25. According to Brian [5], C_p is very nearly the same for the constant flux and the variable flux solutions.

Average values of polarization have been used since, in this analysis, permeation flux has been considered independent of the longitudinal position (see equation 7).

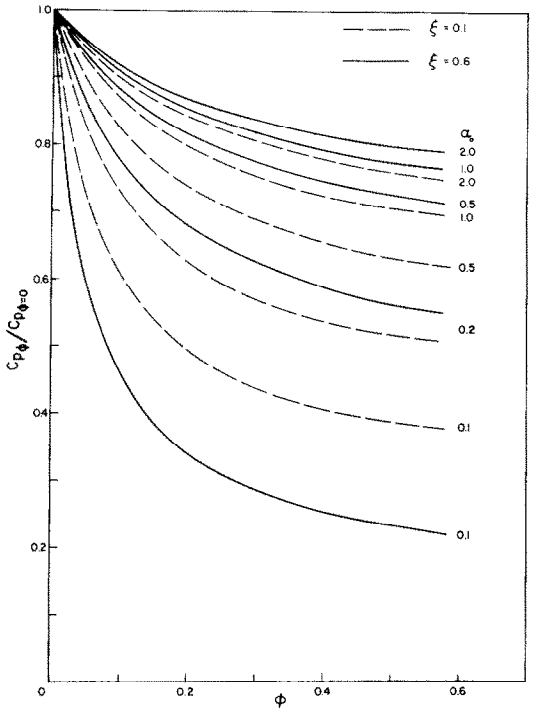

FIG. 10. Effect of slip coefficient on normalized concentration polarization.

Anomalous behavior between experimental results and theoretical analysis based on the steady-state, gel polarization model (GPM) has been reported by Blatt *et al.* [4] and Porter [9]. The flux rates are reported to be 15–30% lower for macromolecules and one to two orders of magnitude less for colloids on the basis of the GPM. The theoretical results in this study have not been compared with experimental data. However, substantial reduction in polarization in the presence of velocity slip strongly indicates one possible reason for the above mentioned anomalous behavior.

The effect of slip coefficient on promoting back diffusion and the fact that slip coefficient is dependent on the surface characteristics of the membrane may suggest different ways of fabricating membranes. As well, the pressure drop along the channel length is reduced with an increase in slip coefficient resulting in reduced pumping requirement and operating costs.

REFERENCES

1. G. S. Beavers and D. D. Joseph, Boundary conditions at a naturally permeable wall, *J. Fluid Mech.* **30**, 197–207 (1967).
2. G. S. Beavers, E. M. Sparrow and R. A. Magnuson, Experiments on coupled parallel flows in a channel and a bounding porous medium, *J. Basic Engng* **92**, 843–848 (1970).
3. A. S. Berman, Laminar flow in channels with porous walls, *J. Appl. Phys.* **24**, 1232–1235 (1953).
4. W. F. Blatt, A. Dravid, A. S. Michaels and L. Nelsen, Solute polarization and cake formation in membrane ultrafiltration: causes, consequences, and control techniques, in *Membrane Science and Technology*, Edited by J. E. Flinn, p. 47. Plenum Press, New York (1970).
5. P. L. T. Brian, Mass transport in reverse osmosis, in *Desalination by Reverse Osmosis*, Edited by U. Merten, p. 161. M.I.T. Press, Cambridge, Mass. (1966).
6. J. P. Kohler, An investigation of laminar flow through a porous-walled channel, Ph.D. Thesis, University of Massachusetts, Amherst (1973).
7. A. S. Michaels, Ultrafiltration, in *Progress in Separation and Purification*, Vol. 1, Edited by E. S. Perry, p. 297. Interscience, New York (1968).
8. A. H. Nayfeh, *Perturbation Methods*. John Wiley, New York (1973).
9. M. C. Porter, Concentration polarization with membrane ultrafiltration, *Ind. Engng Chem. Product Res. Dev.* **11**, 234–248 (1972).
10. D. von Rosenberg, *Methods for the Numerical Solution of Partial Differential Equations*, p. 22. Elsevier, New York (1969).
11. R. Singh and R. L. Laurence, Influence of slip velocity at a membrane surface on ultrafiltration performance—II. Tube flow system, *Int. J. Heat Mass Transfer* **22**, 731–737 (1979).

APPENDIX

(A) *Constants defined in equations* (32) *and* (33)

$$b_1 = -\frac{\chi}{2},$$
$$b_2 = \tfrac{3}{2}\chi(1+2\phi),$$
$$c_1 = \chi^2,$$
$$c_2 = a_2 - a_1,$$
$$c_3 = a_1 - a_3,$$
$$c_4 = \chi^3(9+63\phi+140\phi^2+105\phi^3),$$
$$a_1 = \chi^3(108+756\phi+1680\phi^2+1260\phi^3),$$
$$a_2 = \chi^2(105+420\phi+420\phi^2),$$
$$a_3 = \chi^2(106+420\phi+420\phi^2),$$
$$\chi = \frac{1}{1+3\phi}.$$

(B) *The finite difference solution*

In order to solve equation (20) by a finite difference scheme, a grid is chosen such that $j = 1$ at $\lambda = 0$, $j = 2$ at $\lambda = \Delta\lambda$, $j = 3$ at $\lambda = 2\Delta\lambda$ and so on to $j = NJ$ at $\lambda = 1$. Similarly, $m = 1$ at $\xi = 0$. $\Delta\lambda$ and $\Delta\xi$ are increments in the y and x-directions, respectively. At $j = NJ$, $\lambda = (NJ-1)\Delta\lambda$ and at $m = NM$, $\xi = (NM-1)\Delta\xi$.

The finite difference analogues of derivatives in equation (20) are

$$\left.\frac{\partial^2 C}{\partial\lambda^2}\right|_{j,m} = \frac{C_{j+1,m} - 2C_{j,m} + C_{j-1,m}}{(\Delta\lambda)^2}, \tag{B.1}$$

$$\left.\frac{\partial C}{\partial\lambda}\right|_{j,m} = \frac{C_{j+1,m} - C_{j-1,m}}{2(\Delta\lambda)}, \tag{B.2}$$

$$\left.\frac{\partial C}{\partial\xi}\right|_{j,m} = \frac{C_{j,m} - C_{j,m-1}}{\Delta\xi}. \tag{B.3}$$

Substituting equations (B.1)–(B.3) in equation (20) gives:

$$A_j C_{j-1,m} + B_j C_{j,m} + E_j C_{j+1,m} = F_j C_{j,m-1} = F_j, \quad \text{for } 2 \leqslant j \leqslant NJ-1, \tag{B.4}$$

where

$$A_j = \frac{-V}{2(\Delta\lambda)} - \frac{\alpha_0}{(\Delta\lambda)^2}, \tag{B.5}$$

$$B_j = \frac{U}{\Delta\xi} + \frac{2\alpha_0}{(\Delta\lambda)^2}, \tag{B.6}$$

$$E_j = \frac{V}{2(\Delta\lambda)} - \frac{\alpha_0}{(\Delta\lambda)^2}, \tag{B.7}$$

$$F_j = \frac{U}{\Delta\xi} \cdot C_{j,m-1}. \tag{B.8}$$

Equation (B.4) is implicit in λ with three unknowns $C_{j-1,m}$, $C_{j,m}$ and $C_{j+1,m}$ at the unknown axial distance level m. Using the Taylor series expansion around $j = 1$ and $j = NJ$, boundary conditions, equations (22) and (23), can be written in finite difference form as:

$$C_{1,m} = \tfrac{4}{3}C_{2,m} - \tfrac{1}{3}C_{3,m}, \tag{B.9}$$

$$C_{NJ,m} = \frac{\alpha_0}{[3\alpha_0 - 2(\Delta\lambda)]}(4C_{NJ-1,m} - C_{NJ-2,m}). \tag{B.10}$$

The initial condition, equation (21), is replaced by

$$C_{j,m-1} = 1. \tag{B.11}$$

The above system of simultaneous equations can be represented by a tridiagonal coefficient matrix and is solved most efficiently by the method of Thomas [10]. The solution procedure is as follows:

(1) Start at $m = 2$ and solve for $C_{j,m}$. Form coefficients for $j = 2, \ldots, NJ-1$ and solve for $C_2, \ldots, C_{NJ-1}$ by Thomas. Then, solve for C_1 and C_{NJ} using the boundary conditions, equations (B.9) and (B.10).

(2) Step to next m.

It was found that convergence of the numerical solution was satisfactory for grid size of 0.05 for λ and 0.001 for ξ.

(C) *Thomas algorithm for tridiagonal matrix*

Equation (B.4) is

$$A_jC_{j-1,m} + B_jC_j + E_jC_{j+1,m} = F_j,$$

for $2 \leqslant j \leqslant NJ-1$ with $A_2 = E_{NJ-1} = 0$.

The algorithm is as follows:

$$\beta_j = B_j - \frac{A_jE_{j-1}}{\beta_{j-1}}, \quad \text{with } \beta_2 = B_2, \tag{C.1}$$

and

$$\gamma_j = \frac{F_j - A_j\gamma_{j-1}}{\beta_j}, \quad \text{with } \gamma_2 = \frac{F_2}{B_2}. \tag{C.2}$$

The values of concentrations are then computed backwards from C_{NJ-1}–C_2 as follows:

$$C_{NJ-1,m} = \gamma_{NJ-1} \tag{C.3}$$

and

$$C_{j,m} = \gamma_j - \frac{E_jC_{j+1,m}}{\beta_j}. \tag{C.4}$$

INFLUENCE DE LA VITESSE DE GLISSEMENT, A LA SURFACE D'UNE MEMBRANE, SUR L'ULTRA-FILTRATION—1. SYSTEME D'ECOULEMENT EN CANAL

Résumé—On étudie en détail l'influence de la vitesse de glissement sur une surface poreuse, pour une membrane plane parallèle à un écoulement établi. On examine l'effet du coefficient de glissement sur les profils des vitesses, le gradient de pression et la polarisation de concentration dans l'ultra-filtration. Les équations du mouvement sont résolues par la méthode de perturbation. L'équation de diffusion couplée dans la couche limite est résolue par la méthode des différences finies.

EINFLUSS DER SCHLUPFGESCHWINDIGKEIT AN EINER MEMBRANOBERFLÄCHE AUF DIE ULTRA-FILTRATIONSLEISTUNG I. KANALSTRÖMUNG

Zusammenfassung—Der Einfluß der Schlupfgeschwindigkeit an einer porösen Oberfläche wurde unter der Annahme voll entwickelter Strömung für ein System mit parallelen, ebenen Membranen ausführlich untersucht. Der Einfluß des Schlupfkoeffizienten auf Geschwindigkeitsprofile, Druckgradienten und Konzentrationspolarisation bei Ultrafiltration wurde untersucht. Die Bewegungsgleichungen wurden nach der Methode des regulären Störungsansatzes gelöst. Die gekoppelte Gleichung für die Diffusion in der Grenzschicht wird mittels eines finiten Differenzschemas gelöst.

ВЛИЯНИЕ СКОРОСТИ СКОЛЬЖЕНИЯ НА ПОВЕРХНОСТИ МЕМБРАНЫ НА УЛЬТРАФИЛЬТРАЦИЮ. 1. ТЕЧЕНИЕ В КАНАЛЕ

Аннотация — Проведено детальное исследование влияния скорости скольжения на пористой поверхности в системе параллельных плоских мембран на ультрафильтрацию при допущении, что течение является полностью развитым. Исследовано влияние коэффициента скольжения на профили скорости, градиент давления и распределение концентрации при ультрафильтрации. Уравнения движения решены методом регулярных возмущений. Взаимосвязанное уравнение диффузии в пограничном слое решается с помощью конечно-разностной схемы.